NON-LINEAR AUTO-PARAMETRIC STABILITY LOSS OF A SLENDER STRUCTURE DUE TO RANDOM NON-STATIONARY SEISMIC EXCITATION

J. Náprstek[1] and C. Fischer[1]

[1]*Dr., Institute of Theoretical and Applied Mechanics ASCR v.v.i., Prague, Czech Republic*
E-mail: {naprstek, fischerc}@itam.cas.cz

ABSTRACT:

Slender structures exposed to a strong vertical component of an earthquake excitation are endangered by auto-parametric resonance effect. This highly non-linear dynamic process caused heavy damages or collapses of towers, bridges and other structures in the past. In sub-critical linear regime vertical and horizontal response components are independent and therefore no horizontal response component is observed. If an amplitude of the vertical excitation in a structure foundation exceeds a certain limit, a vertical response component looses stability and dominant horizontal response components arise. This post-critical regime (auto-parametric resonance) follows from the non-linear interaction of vertical and horizontal response components and can lead to a failure of the structure. The seismic type broadband random non-stationary excitation can be particularly dangerous in this connection. The paper tries to bring a qualitative assessment of this process using three-DOF theoretical model respecting dynamic properties of the structure and its subsoil including internal viscosity.

KEYWORDS: dynamic stability, auto-parametric response, non-linear dynamics, semi-trivial solution, post-critical response.

1. INTRODUCTION

Many studies devoted to dynamics of slender structures (towers, masts, chimneys, bridges, etc.) related with earthquake attack have been published. They are dealing predominantly with an influence of horizontal excitation components. On the other hand a strong vertical excitation component especially in the earthquake epicentrum area can be decisive. The vertical component of the subsoil movement caused heavy damages or collapses of many high rise structures due to earthquake attack. Very widely used linear approach, however, usually doesn't provide any interesting knowledge in such a case. It reveals that the origin of these problems consists in auto-parametric resonance effects. This non-linear dynamic process in a post-critical regime caused heavy damages or collapses of many towers, bridges and other structures due to earthquake attack.

In subcritical linear regime the vertical and horizontal response components are independent. If no horizontal excitation is taken into account no horizontal response component is observed. The semi-trivial solution gives a full image of the structure behavior. If an amplitude of a vertical harmonic excitation in a structure foundation exceeds a certain limit, vertical response looses its dynamic stability and a dominant horizontal response component through the non-linear interaction of both component is generated. Therefore the system has a character of the auto-parametric system.

Auto-parametric systems have been intensively studied for the last three decades. These investigations are motivated by various technical branches and by basic theoretical research in rational mechanics. A theoretical outline dealing with these systems has been presented probably for the first by Haxton & Barr (1974). During this time many papers contributing to analytical, numerical as well as experimental aspects of auto-parametric systems have been published mostly by Tondl, Nabergoj and co-authors, e.g. (1991, 1994a, 1994b, 1997, 2000). Many other references can be found. Several monographs, e.g. Hatwal, Mallik & Ghosh (1983) or Guckenheimer & Holmes (1983), presenting a comprehensive overview of partial results and methods have appeared. A couple of papers dealing with auto-parametric systems under deterministic and random excitation has been recently published by Náprstek and co-authors (1998, 2002, 2007).

Let us consider the three DOF theoretical model outlined in the Figure 1. The system is Hamiltonian, e.g. Arnold (1978). To deduce the governing differential system in the form of Lagrange equations the kinetic and potential energies of the moving system are formulated as follows:

$$\begin{aligned} T &= \tfrac{1}{2}(M+m)\dot{y}^2 + \tfrac{1}{2}Mr^2\dot{\varphi}^2 - m\dot{y}(l\dot{\varphi}+\dot{\xi})\sin\varphi + \tfrac{1}{2}m(l\dot{\varphi}+\dot{\xi})^2 & (a) \\ U &= (M+m)gy - mg[l(1-\cos\varphi)+\xi\sin\varphi] + \tfrac{1}{2}C(y-y_0)^2 + \tfrac{1}{2}Cr^2\varphi^2 + 3EJ/l^3\cdot\xi^2 & (b) \end{aligned} \quad (1.1)$$

$y = y(t)$ - vertical displacement of the B point;
$y_0 = y_0(t)$ - kinematic excitation (seismic random process);
$\varphi = \varphi(t)$ - angular rotation of the system in the B point;
$\xi = \xi(t)$ - bending deformation of the vertical console;
M, m - foundation and structure effective masses;
C, EJ - subsoil stiffness, console bending stiffness;
η_c, η_e - viscous components of the C, EI stiffness (Kelvin);
ϱ, l - geometric parameters.

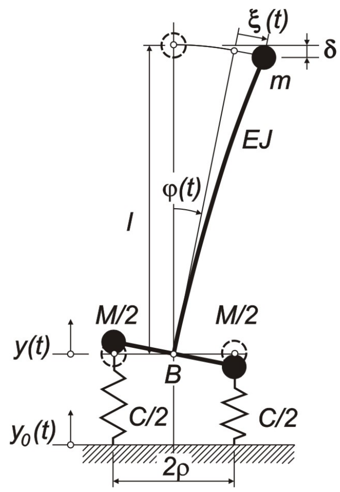

Figure 1: Outline of a 3-DOF auto-parametric system.

Non-dimensional response and excitation components

$$\zeta_0 = y_0/l,\ \zeta = y/l,\ \varphi,\ \psi = \varphi + \xi/l \quad (1.2)$$

are useful to be introduced. When the Lagrange equations are deduced the approximation reflecting an early post-critical state can be adopted:

$$\sin\varphi \approx \varphi\ ; \quad \cos\varphi \approx 1 \quad (1.3)$$

The governing 3DOF differential system can be formulated as follows:

$$\begin{aligned} \ddot{\zeta} - \kappa_0(\dot{\psi}\varphi)^{\bullet} + \omega_0^2(\zeta - \zeta_0 + \eta_c(\dot{\zeta}-\dot{\zeta}_0)) &= 0, & (a) \\ \ddot{\varphi} - \kappa_1(\dot{\zeta}\varphi)^{\bullet} + \kappa_1\ddot{\psi} + \kappa_1\dot{\zeta}\dot{\psi} - \kappa_1\omega_2^2\psi + \omega_1(\varphi + \eta_c\dot{\varphi}) &= 0, & (b) \\ \ddot{\psi} - (\dot{\zeta}\varphi)^{\bullet} + \omega_3^2(\psi - \varphi + \eta_e(\dot{\psi}-\dot{\varphi})) &= 0, & (c) \end{aligned} \quad (1.4)$$

where following notation has been used:

$$\begin{aligned} &\kappa_0 = \frac{m}{M+m}\,, \qquad \kappa_1 = \frac{m\cdot l^2}{M\cdot\varrho^2}\,, \\ &\omega_0^2 = \frac{C}{M+m}\,, \qquad \omega_1^2 = \frac{C}{M}\,, \qquad \omega_2^2 = \frac{g}{l}\,, \qquad \omega_3^2 = \frac{6EJ}{m\cdot l^3}\,. \end{aligned} \quad (1.5)$$

Concerning the excitation process $\zeta_0(t)$, it will be considered as harmonic in the first step. Later the random non-stationary character of $\zeta_0(t)$ will be respected as a product of a deterministic amplitude modulating function and a stationary random process of Kanai-Tajimi type.

2. SEMI-TRIVIAL SOLUTION AND ITS STABILITY

Let us consider the harmonic excitation transformed into the dimensionless form:

$$y_0 = A_0\sin\omega t \quad \Rightarrow \quad \zeta_0 = a\sin\omega t\,, \quad A_0 = a_0\cdot l \quad (2.1)$$

and assume that the stationary semi-trivial solution exists. Its general form can be written as follows:

$$\zeta_s = a_c\cdot\cos\omega t + a_s\cdot\sin\omega t\,, \quad \psi = 0\,, \quad \varphi = 0 \quad (2.2)$$

Substituting Eqs (2.2) into the system (1.4), Eqs (1.4b) and (1.4c) are satisfied identically, while Eqn. (1.4a) provides the coefficients a_c, a_s doing obvious modifications:

$$a_c = -\frac{a_0\omega_0^2}{\delta}\omega^3\eta_c\ , \quad a_s = \frac{a_0\omega_0^2}{\delta}(\omega_0^2 - \omega^2 + \omega_0^2\omega^2\eta_c^2)\ , \quad \delta = (\omega^2 - \omega_0^2)^2 + \omega_0^4\omega^2\eta_c^2 \tag{2.3}$$

Expression (2.2) together with coefficients (2.3) represents an approximate simple linear stationary solution of the SDOF system moving in vertical direction being excited kinematically in the point B. The resonance curve of the response amplitude has the form:

$$R_0^2 = a_c^2 + a_s^2 = \frac{a_0^2\omega_0^4}{\delta}(1 + \omega^2\eta_c^2) \tag{2.4}$$

which can be seen in the Figure 2. However the solution being characterized by this curve can be unstable beyond a certain value of the excitation amplitude a_0 in some intervals of the excitation frequency ω. For this reason the stability analysis must be carried out. Dynamic stability of non-linear systems with a couple of degrees of freedom has been discussed using various methods by many authors, e.g. Benettin et al. (1980), Tondl (1991), or Bajaj et al. (1994).

Let us adopt the linear perturbation approach in order to assess the stability limits of the semi-trivial solution (2.2). Hence it can be written approximately in the arbitrarily small neighborhood of the semi-trivial solution:

$$\begin{array}{rclclcll}
\zeta(t) & = & \zeta_s(t) & + & r(t) & = & \zeta_s(t)\ +\ r_c(t)\cos\omega t + r_s(t)\sin\omega t\ , & (a) \\
\varphi(t) & = & 0 & + & p(t) & = & p_c(t)\cos\tfrac{1}{2}\omega t + p_s(t)\sin\tfrac{1}{2}\omega t\ , & (b) \\
\psi(t) & = & 0 & + & s(t) & = & s_c(t)\cos\tfrac{1}{2}\omega t + s_s(t)\sin\tfrac{1}{2}\omega t\ . & (c)
\end{array} \tag{2.5}$$

The argument (t) will be omitted in further text where possible $(\zeta, \varphi, \psi, r, r_c, r_s, ...)$ etc. Introducing expression (2.5a) into Eqn. (1.4a) and taking into account that ζ_s represents its semi-trivial solution, following equation for perturbation r can be extracted:

$$\ddot{r} + \omega_0^2(r + \eta_c\dot{r})\ =\ 0 \tag{2.6}$$

Eqn. (2.6) is linear and homogeneous. It is obvious that $\lim_{t\to\infty} r_c, r_s\ =\ 0$ and stationary solution vanishes. For this reason the vertical response component ζ remains independent and stable in the neighborhood of the semi-trivial solution ζ_s (on the level of the linear perturbation approach). Let us put now the second column of the expressions (2.5a-c) into Eqs (1.4b,c). Keeping only the linear terms of perturbations p, s and respecting that $r \equiv 0$ one obtains the following differential system:

$$\begin{array}{ll}
\ddot{p}\ + (\kappa_1\omega_3^2\eta_e + \omega_1^2\eta_c)\dot{p}\ - \kappa_1(\omega_3^2\eta_e - \dot{\zeta}_s)\dot{s}\ + (\kappa_1\omega_3^2 + \omega_1^2)p\ - \kappa_1(\omega_2^2 + \omega_3^2)s\ =\ 0 & (a) \\
\ddot{s}\ - (\omega_3^2\eta_e + \dot{\zeta}_s)\dot{p}\ + \omega_3^2\eta_e\dot{s}\ - (\omega_3^2 + \ddot{\zeta}_s)p\ + \omega_3^2 s\ =\ 0 & (b)
\end{array} \tag{2.7}$$

The system (2.7) is linear as well. However three coefficients include harmonic components due to $\ddot{\zeta}_s, \dot{\zeta}_s$ terms being given by Eqn. (2.2). The system (2.7) is of the Mathieu type and its solution stability should be verified.

As the next step functions p, s in Eqs (2.7) should be replaced by means of their first harmonics represented by the third column in Eqs (2.5a-c). The method of harmonic balance enables to obtain the following homogeneous algebraic system for p_c, p_s, s_c, s_s parameters:

$$\begin{bmatrix}
-\frac{\omega^2}{4} + (\kappa_1\omega_3^2 + \omega_1^2), & \frac{1}{2}(\kappa_1\omega_3^2\eta_e + \omega_1^2\eta_c), & -\kappa_1(\omega_2^2 + \omega_3^2)\ +\kappa_1\frac{\omega^2}{4}a_c, & -\frac{1}{2}\kappa_1\omega_3^2\eta_e\ +\kappa_1\frac{\omega^2}{4}a_s \\
-\frac{1}{2}(\kappa_1\omega_3^2\eta_e + \omega_1^2\eta_c), & -\frac{\omega^2}{4} + (\kappa_1\omega_3^2 + \omega_1^2), & \frac{1}{2}\kappa_1\omega_3^2\eta_e\ +\kappa_1\frac{\omega^2}{4}a_s, & -\kappa_1(\omega_2^2 + \omega_3^2)\ -\kappa_1\frac{\omega^2}{4}a_c \\
-\omega_3^2\ + \frac{\omega^2}{4}a_c, & -\frac{1}{2}\omega_3^2\eta_e\ + \frac{\omega^2}{4}a_s, & -\frac{1}{4}\omega^2 + \omega_3^2, & \frac{1}{2}\omega\omega_3^2\eta_e \\
\frac{1}{2}\omega_3^2\eta_e\ + \frac{\omega^2}{4}a_s, & -\omega_3^2\ - \frac{\omega^2}{4}a_c, & -\frac{1}{2}\omega\omega_3^2\eta_e, & -\frac{1}{4}\omega^2 + \omega_3^2
\end{bmatrix}
\begin{bmatrix} p_c \\ p_s \\ s_c \\ s_s \end{bmatrix} = 0 \tag{2.8}$$

Let us be conscious that Eqn. (2.8) is meaningful only under certain conditions. The system response should be fully or at least nearly stationary in order to be entitled to apply the harmonic balance method. In other words functions p_c, p_s, s_c, s_s should enable to be approximated by constants within the interval of one period or at least to be considered as functions of the "slow time". Under circumstances of a chaotic or quasi-periodic response with noticeable energy transfer between ζ and φ, ψ components, the harmonic balance method is inapplicable and the system (2.8) becomes meaningless.

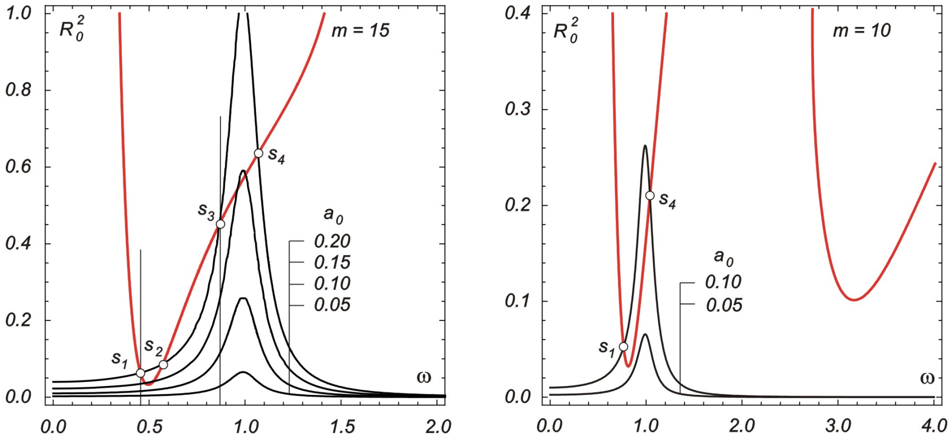

Figure 2: Relation of resonance curves (black) and stability limits (red); left picture: $M = 3990, m = 15, \eta_c = 0.2, \eta_e = 0.2, l = 20, g = 9.81, EJ = 10000, C = 4000 > gml/r^2 = 2943$; $a_0 = 0.2 \Rightarrow s_1 = 0.4548, s_2 = 0.5718, s_3 = 0.8671, s_4 = 1.0680$; right picture: $m = 10; C = 4000 > gml/r^2 = 1962$; $a_0 = 0.1 \Rightarrow s_1 = 0.7652, s_4 = 1.0396$.

If the above general condition is complied with, p_c, p_s, s_c, s_s can be taken as parameters. The system (2.8) being homogeneous cannot provide non-trivial solution unless the determinant of its matrix vanishes. The respective determinant can be evolved with respect to R_0^2 amplitude and written in the form of the scalar homogeneous equation:

$$\begin{aligned}
&R_0^4\left\{\ \kappa_1^2\omega^8\right\}- \\
&-R_0^2\left\{\ 2\omega^4\kappa_1\left[\omega^4+8\kappa_1\omega_2^4-4\omega_3^2(\omega^2+\kappa_1(\omega^2-4\omega_2^2))+\right.\right. \\
&\qquad\left.\left.+8\kappa_1\omega_3^4(4+\omega^2\eta_e^2)+4\omega_1^2(-\omega^2+\omega_3^2(4+\omega^2\eta_c\eta_e))\right]\right\}+ \\
&+\left\{\ \omega^8-8\omega_3^2(\omega^6+\kappa_1(\omega^6+4\omega^4\omega_2^2))+4\omega_3^4(4+\omega^2\eta_e^2)(\omega^2+\kappa_1(\omega^2+4\omega_2^2))^2+\right. \\
&\qquad+4\omega_1^4(4+\omega^2\eta_c^2)(\omega^4-8\omega^2\omega_3^2+4\omega_3^2(4+\omega^2\eta_e^2))+ \\
&\left.+8\omega_1^2\ \left[-\omega^6+\omega_3^2(8\omega^4+\omega^2\kappa_1(4+\omega^2\eta_c\eta_e)(\omega^2+4\omega_2^2))-4(4+\omega^2\eta_e^2)(\omega^2+\kappa_1\omega_3^4(\omega^2+4\omega_2^2))\right]\right\}\ =\ 0
\end{aligned} \tag{2.9}$$

Eqn. (2.9) represents a quadratic equation for R_0^2. Only real positive solution is useful. Negative or complex conjugate roots should be avoided. Conditions for parameters (1.5) and variable frequency ω could be carried out to fulfil these requests. Consequently $R_0^2 > 0$ as a function of ω consists in a general case either of two or one branches or doesn't exist. Two typical examples have been plotted in the Figure 2 (the left picture is a more detailed and a larger scaled yellow item in the Figure 3).

Resonance curves for a few excitation amplitudes a_0 are plotted in black while the stability limits described by the Eqn. (2.9) are shown in red color for a set of fixed parameters of the system (all parameters used are written in the caption). Points s_1, s_2 and s_3, s_4 in the left picture represent lower and upper limits of intervals where the semi-trivial solution becomes instable and post-critical response should be investigated. It is obvious that the most sensitive interval where the stability loss can be expected is in the domain of the basic eigen frequency ω_0 as we can see in the left picture - interval $\omega\epsilon(s_3, s_4)$ and also in the right picture - interval $\omega\epsilon(s_1, s_4)$. However the stability limit indicates also another instability interval $\omega\epsilon(s_1, s_2)$ in lower frequency range. This fact is related with a hypothetic "eigen frequency" in the component φ. The right picture demonstrates two separate parts of the particular stability limit.

In order to get a certain overview regarding the influence of basic parameters m (mass of the structure) and C (stiffness of the subsoil) on the stability loss, dynamic response and other properties of the system for various sets of input parameters have been evaluated. Respective results are summarized in Figures 3 (increasing $m\epsilon(10, 160)$) and in Figure 4 (increasing $C\epsilon(1000, 15000)$). With increasing m a certain drop of system sensitivity in the area

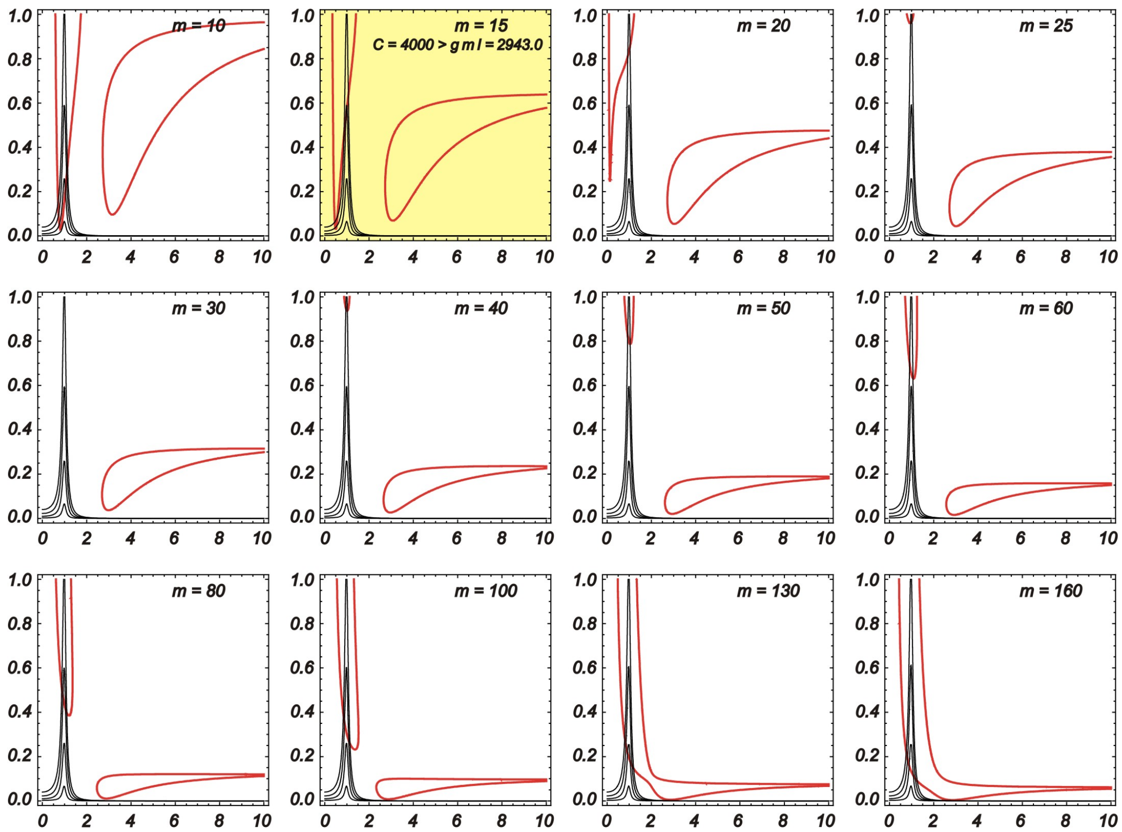

Figure 3: Resonance curves (black) and stability limits (red) for an increasing value of the mass $m\epsilon(10; 180)$.

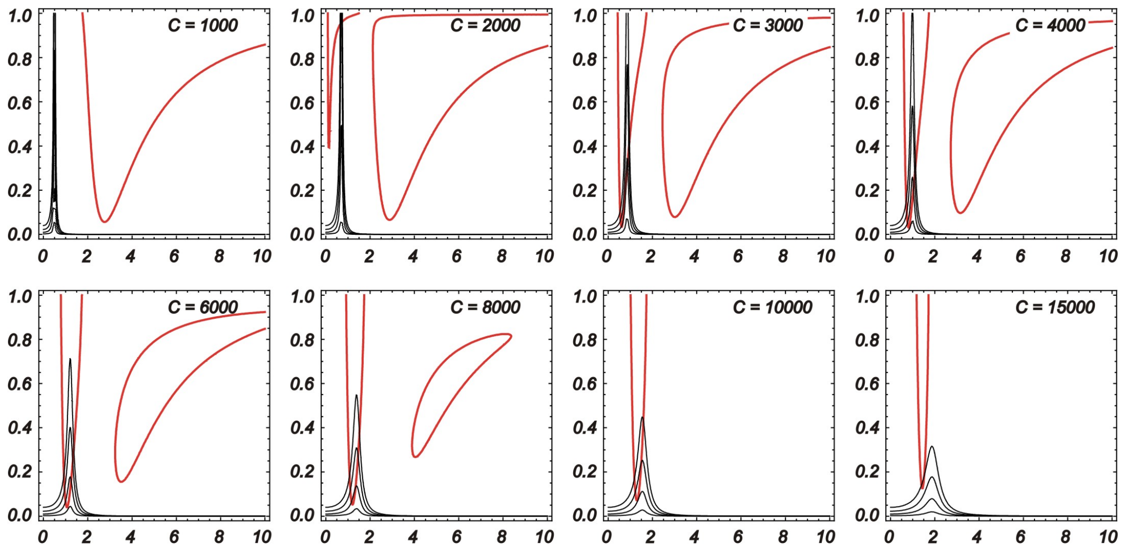

Figure 4: Resonance curves (black) and stability limits (red) for an increasing value of the spring stiffness $C\epsilon(1000; 15000)$.

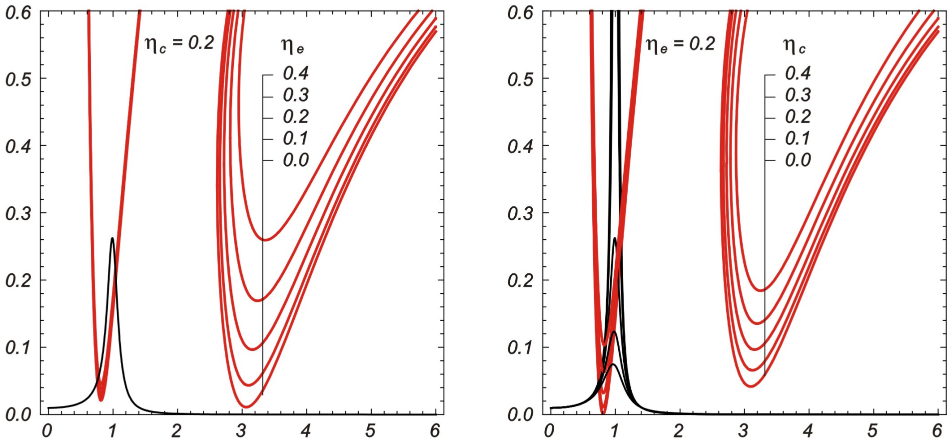

Figure 5: Influence of the viscous damping on the stability limits (red curves); left picture: spring viscosity η_c fixed, viscosity of the vertical deformable console $\eta_e \epsilon (0, 0.4)$ increasing; right picture: $\eta_c \epsilon (0, 0.4)$ increasing, η_e fixed.

of ω_0 against the stability loss is evident $m \epsilon (10, 30)$. The size of the secondary instability area is also decreasing in the same time. Starting at $m = 30$ the resonance domain ω_0 gains importance once again and for $m > 100$ both instability domains join together. Although the cases for $m > 25$ demonstrated in Figure 3 are rather beyond the static stability and consequently their interpretation can be problematic, this series provides an obvious warning against an existence of an upper limit of m when other parameters remain fixed.

Just opposite tendency can be noted when increasing the stiffness C. The successive disappear of the secondary instability area with increasing C is obvious. Taking into account the drop of the resonance curve in the resonance domain, one should conclude that increase of C stiffness contributes to the system stabilization.

Let us draw our attention to the influence of the internal damping. Two types of the damping have been taken into account in the basic mathematical model. The first one being quantified by η_c influences strongly the semi-trivial solution and the resonance curve shape, see Figure 5. The right part demonstrates the system sensitivity to η_c especially in the ω_0 area. Concerning the left part of Figure 5, we can see that the vertical console viscosity from intelligible reasons is applicable only after the stability loss in the post-critical regime. Therefore position and extent of the instability domain is very weekly influenced by the parameter η_e. Concerning the secondary instability area they are not very different regardless whether η_c or η_e is altered within the interval indicated.

3. POST-CRITICAL SYSTEM RESPONSE

In order to demonstrate the system behavior in frequency intervals of stable and instable semi-trivial solution, several numerical simulations using the governing differential system (1.4) have been done. The input data correspond with those providing results plotted in Figure 2 (left picture). Results of simulations are depicted in Figure 6. In the right column the vertical response component $\zeta(t)$ in dimensionless form, see Eqs (1.2), is presented. In the left column both $\varphi(t)$ (blue) and $\psi(t)$ (red) response components are plotted. The excitation amplitude is always $a_0 = 0.2$.

The time history of the system response for the excitation frequency $\omega = 0.4$ is demonstrated in the row (a). The semi-trivial response is stable despite of a small initial deviation of ψ component. Components $\varphi(t), \psi(t)$ are approaching asymptotically to zero. A transitional state and a beginning of the post-critical state is visible in the row (b) where holds $\omega = s_1$. The noticeable increase of $\varphi(t), \psi(t)$ components within the interval $\omega \epsilon (s_1, s_2)$ is obvious in the rows (c,d), while $\zeta(t)$ still remains on a similar level. Amplitudes of $\varphi(t), \psi(t)$ are approaching to certain horizontal asymptotes for $t \to \infty$. There is a question if such an increase of the horizontal component of the system response is admissible for the structure with respect to various regulations. Overcoming s_2, the semi-trivial response is re-established and $\varphi(t), \psi(t)$ vanish once again, although vertical component ζ significantly grows up, rows (e-h). Finally in the row (i) very dramatic post-critical system response in the interval $\omega \epsilon (s_3, s_4)$ is obvious, nevertheless $\varphi(t), \psi(t)$ are still approaching to a certain horizontal asymptote. In the row (j) the stable semi-trivial

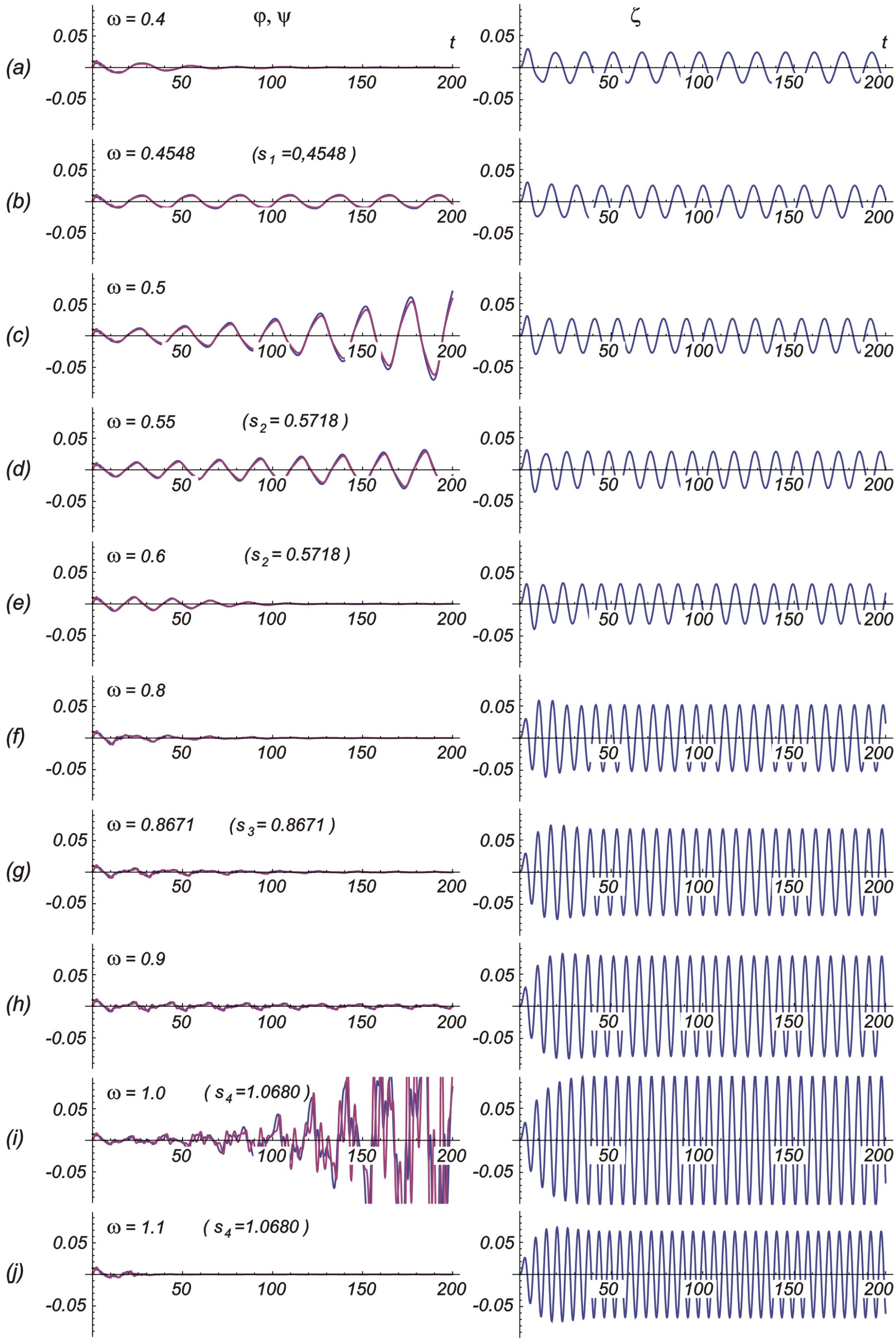

Figure 6: Time history of the system response; left column: $\varphi(t)-$ blue, $\psi(t)-$ red (post-critical response components); right column: $\zeta(t)$ blue (vertical response component in the point B); limits of semi-trivial solution stability/instability: $s_1 = 0.4548, s_2 = 0.5718, s_3 = 0.8671, s_4 = 1.0680$.

solution without any horizontal components for any arbitrary $\omega > s_4$ arises.

Let us notice that the dynamic stability limits are influenced by the bending stiffness EJ of the vertical console very weakly. However the system response in the post-critical state in particular $\varphi(t), \psi(t)$ components are influenced by this parameter significantly, see Figure 6, rows (c,i).

4. CONCLUSION

Non-linear auto-parametric system with three degrees of freedom has been investigated. The aim of this study was to compose a simple mathematical model which enables to assess the nonlinear post-critical dynamic response of a slender vertical structure on an elastic subsoil exposed to strong vertical excitation. The existence of certain intervals of the excitation frequency has been proved where semi-trivial solution loses its dynamic stability and strong horizontal response components become decisive from the point of view of various standards. In post-critical state mainly bending effects in the structure foundation and deformability of the vertical console are dominant. Various forms and internal structure of stability limits with respect to principal system parameters have been found.

ACKNOWLEDGMENTS: The kind support of the Czech Scientific Foundation No. 103/06/0099, Grant Agency of the ASCR No. A2071401, A200710505 and AV 0720710524 research plan are gratefully acknowledged.

REFERENCES

Arnold V.I. (1978) *Mathematical Methods of Classical Mechanics*. Springer, New York.

Bajaj A.K., Chang S.I., Johnson J.M. (1994) Amplitude modulated dynamics of a resonantly excited autoparametric two degree of freedom system. *Nonlinear dynamics*, 5, 433-457.

Benettin G., Galgani L., Giorgilli A., Strelcyn M. (1980) Lyapunov characteristic exponents for smooth dynamical systems and Hamiltonian systems: A method for computing all of them. Part 2, Numerical application. *Meccanica*, 15, 21.

Guckenheimer J., Holmes P. (1983) *Nonlinear Oscillations, Dynamical Systems and Bifurcations of Vector Fields*. Springer, New York.

Hatwal H., Mallik A.K., Ghosh A. (1983) Forced nonlinear oscillations of an autoparametric system. *ASME Jour. Applied Mechanics*, 50, 657-662, 3.

Haxton R.S., Barr A.D.S. (1974) The autoparametric vibration absorber. *ASME Jour. Applied Mechanics*, 94, 119-125.

Nabergoj R., Tondl A. (1994a) A simulation of parametric ship rolling: Effects of hull bending and torsional elasticity. *Nonlinear Dynamics*, 6, 265-284.

Náprstek J. (1998) Non-linear self-excited random vibrations and stability of an SDOF system with parametric noises. *Meccanica*, 33, 267-277.

Náprstek J., Pirner M. (2002) Non-linear behaviour and dynamic stability of a vibration spherical absorber. In: *Proc. 15th ASCE Engineering Mechanics Division Conference* (A. Smyth et al. eds). Columbia Univ., New York, 10 pp. CD ROM.

Náprstek J., Fischer C. (2007) Auto-parametric semi-trivial and post-critical response of a spherical pendulum damper. In: *Proc. 11th Int.Conf. on Civ.Struct.Env. Engineering Computing* (B.H.V. Topping edt.). Civil-Comp Press, Malta St.Julian, 2007, CD paper #CC2007/2006/0020, 18 pgs.

Tondl A. (1991) *Quenching of Self-Excited Vibrations*. Academia, Prague.

Tondl A., Nabergoj R. (1994b) Non-periodic and chaotic vibrations in a flow induced systems. *Chaos, Solitons and Fractals*, vol. 4, 12: 2193-2202.

Tondl A. (1997) To the analysis of autoparametric systems. *Z. Angew. Math. Mech.*, vol77, 6, 407-418.

Tondl A., Ruijgrok T., Verhulst F., Nabergoj R. (2000) *Autoparametric Resonance in Mechanical Systems*. Cambridge University Press, Cambridge.